THE JOURNAL OF PHYSICAL CHEMISTRY LETTERS
A JOURNAL OF THE AMERICAN CHEMICAL SOCIETY

pubs.acs.org/JPCL

Letter

Could Irradiation Introduce Oxidized Oxygen Signals in Resonant Inelastic X-ray Scattering of Battery Electrodes?

Qingtian Li, Zachary W. Lebens-Higgins, Yixuan Li, Ying Shirley Meng, Yi-de Chuang, Louis F. J. Piper,* Zhi Liu,* and Wanli Yang*

Cite This: *J. Phys. Chem. Lett.* 2021, 12, 1138−1143

Read Online

ACCESS | Metrics & More | Article Recommendations

ABSTRACT: The characterization of oxidized oxygen states through high-efficiency mapping of resonant inelastic X-ray scattering (mRIXS) has become a crucial approach for studying the oxygen redox activities in high-energy battery cathodes. However, this approach has been recently challenged due to the concern of irradiation damage. Here we revisited a typical Li-rich electrode, $Li_{1.144}Ni_{0.136}Mn_{0.544}Co_{0.136}O_2$, in both lithiated and delithiated states and evaluated the X-ray irradiation effect in the lengthy mRIXS experiments. Our results show that irradiation cannot introduce any oxidized oxygen feature, and the features of oxidized oxygen are weakened with a high X-ray dose. The results confirm again that mRIXS detects the intrinsic oxidized oxygen state in battery electrodes. However, the distinct irradiation effects in different systems imply that irradiation could selectively target the least stable elemental or chemical states, which should be analyzed with caution in the study of active chemical states.

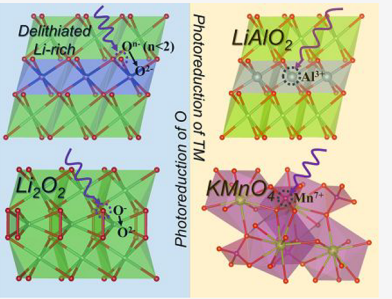

The need for modern sustainable energy applications, especially electric vehicles, has triggered a pressing demand to improve the capacity and energy density of batteries. As the bottleneck of battery capacity, transition-metal (TM) oxide-based battery cathodes have been under intensive studies for high-capacity and high-voltage operations, which often trigger redox activities beyond the traditional TM redox reactions, that is, oxygen redox reactions.[1−4] The concept of utilizing a reversible oxygen redox, however, was formalized much later than it was first discussed.[2,3] This is partially because the oxygen activities during high-voltage electrochemical cycling typically involve irreversible oxygen release and surface reactions, which are often entangled with the practically meaningful reversible oxygen redox reaction.[5] Even since the oxygen redox concept evolved into an active research topic, fervent debates on the reliable characterization of the lattice oxygen redox have never been settled. For example, early works based on X-ray photoelectron spectroscopy (XPS) and, later, high-energy hard XPS have been found to be questionable due to the limitation on the probe depth and the effects from TMs.[6] Signals from another popular technique, oxygen K-edge (O-K) X-ray absorption spectroscopy (XAS), have been found to be dominated by TM states hybridized with O, in both its intensity and line shape.[7] Therefore, a reliable technique for detecting the intrinsic oxygen oxidation state regardless of its form in TM oxides has become a critical challenge.

The complication of detecting oxygen states in TM oxides largely stems from the strong hybridization between the TM and O in these battery compounds. Actually, O-K XAS is usually sensitive to detect different chemical states in molecular or organic systems, including the differences between the O^{2-}, O^{1-}, and O^0 states;[8,9] however, the strong TM effect on the O-K XAS spectra through TM-O hybridization easily conceals the possible oxidized oxygen signals in oxide electrodes.[7,10] Therefore, the key technical challenge for detecting the intrinsic oxidized oxygen state is to separate its signature from the strong TM-O hybridization signals that are largely of TM nature.[7] Fortunately, high-efficiency mapping of resonant inelastic X-ray scattering (mRIXS) has been developed and has been shown to be able to solve this technical challenge by resolving the energies of the emitted photons, that is, the emission energy, at each excitation energy across the absorption edge.[11,12] Two groups of mRIXS features are associated with the oxidized oxygen state in oxide cathodes: (i) a relatively sharp feature around the 531 eV excitation energy and 523 to 524 eV emission energy[10,11,13−15] and (ii) an enhanced feature with low energy loss close to the elastic line at the same excitation energy.[16,17] These features resemble the reference signals of peroxide and O_2.[18,19] A number of mRIXS and RIXS works have been reported to clarify the existence or nonexistence of lattice oxygen redox reactions in both Li-ion

Received: December 10, 2020
Accepted: January 14, 2021

https://dx.doi.org/10.1021/acs.jpclett.0c03639
J. Phys. Chem. Lett. 2021, 12, 1138−1143

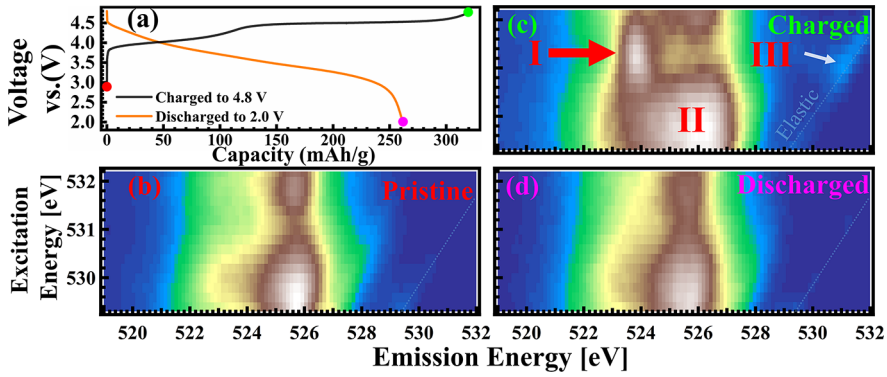

Figure 1. (a) Typical electrochemical profile of $Li_{1.144}Ni_{0.136}Mn_{0.544}Co_{0.136}O_2$ versus Li counter electrode. Three representative samples in different states of charge were selected for O K-edge mRIXS measurements. (b–d) O-K mRIXS of three electrodes: pristine electrode (lithiated), electrode charged to 4.8 V (delithiated), and electrode discharged to 2.0 V (lithiated). Data were collected with 4.5×10^{11} pps X-ray beam flux with sample itinerary throughout the data collection.

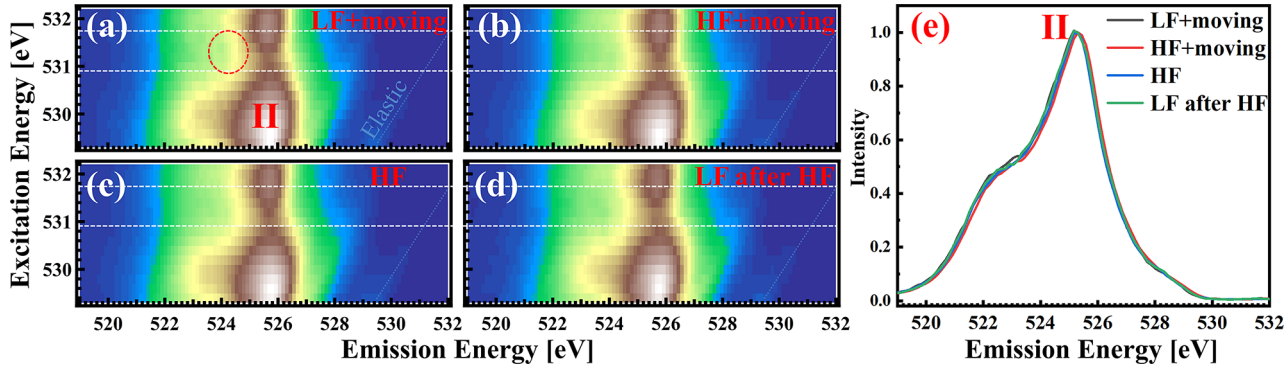

Figure 2. (a–d) O K-edge mRIXS of the pristine $Li_{1.144}Ni_{0.136}Mn_{0.544}Co_{0.136}O_2$ electrode at four different irradiation exposure conditions: (a) low X-ray flux (4.5×10^{11} pps) with sample rastering (LF + moving), (b) high flux (2.0×10^{12} pps) with sample rastering (HF + moving), (c) high flux with stationary sample (HF), and (d) low flux with the same sample position as that for panel c (LF after HF). The red dashed circle in panel a indicates the energy position of the signature of oxidized oxygen. (e) Integrated mRIXS intensity within the energy window of 530.9 to 531.7 eV excitation energies (between the dashed white lines). The spectra are all normalized by peak (II) for direct comparisons.

and Na-ion, both Li-rich and conventional, and both layered and rocksalt materials.[13−15,20−31]

However, the reliability of the RIXS findings on the oxidized oxygen state has recently been strongly denied by a proposal of a redox reaction mechanism based on Mn^{7+} in Li-rich materials, in which, the radiation damage effect is proposed to be one of the reasons for the observed oxidized oxygen features.[32] The concern was aroused from observations of the oxidized oxygen feature $LiAlO_2$ due to radiation damage.[33,34] Another high Mn valence system, $KMnO_4$, displays the same kind of behavior with emerging features of oxidized oxygen upon irradiation.[35] However, Li_2O_2 under soft X-ray irradiation displays an oxygen reduction process into Li_2O.[8] Additionally, we previously showed that the oxidized oxygen feature intensity in quick RIXS cuts is reduced upon X-ray dose.[34] These debates and distinct behaviors make it necessary to evaluate the irradiation effect in the lengthy mRIXS of the oxygen redox states.

In this work, we re-evaluated the irradiation effect of the mRIXS of a standard Li-rich electrode, $Li_{1.144}Ni_{0.136}Mn_{0.544}Co_{0.136}O_2$, at both lithiated (discharged) and delithiated (charged) states. Our results unambiguously show that irradiation cannot introduce any oxidized oxygen feature in the electrode that has no oxidized oxygen species. For the charged electrode with oxidized oxygen, slow mRIXS displays the same trend upon radiation dose as the quick RIXS scans, that is, the oxidized oxygen signals drop upon the X-ray dose. Keeping the sample moving back and forth (rastering) during experiments could largely ease the radiation damage, even at a high dose level. Therefore, mRIXS could, at most, underestimate the oxygen redox states in battery cathodes if the flux was not carefully controlled. Our results settle the debate on the reliability of mRIXS findings of oxygen redox states in battery electrodes. Additionally, we provide the rationality behind the distinct irradiation effects between the different materials, $LiAlO_2$, $KMnO_4$, Li_2O_2, and battery electrodes.

The synthesis, structural characterizations, and electrochemical cycling of $Li_{1.144}Ni_{0.136}Mn_{0.544}Co_{0.136}O_2$ were reported previously.[34] The electrodes measured here were cycled in a voltage range of 2–4.8 V at a rate of 0.05 C (12.5 mAh/g). O-K mRIXS was collected at room temperature, but liquid N_2 cooling was tested with no effect. Technical details and air-free sample handling have been reported previously.[12,13] X-ray flux is controlled by setting the beamline slits to 35 and 70 μm, with flux of around 4.5×10^{11} (low flux mode, LF) and 2.0×10^{12} (high flux mode, HF) photons per second (pps), respectively. Note that the LF mode has been our typical setting for studying battery materials, and the latter is the upper limit of our RIXS experiments before the energy resolution is lost. For direct comparisons, the data collection time of each mRIXS map, regardless of the low-flux or high-

https://dx.doi.org/10.1021/acs.jpclett.0c03639
J. Phys. Chem. Lett. 2021, 12, 1138−1143

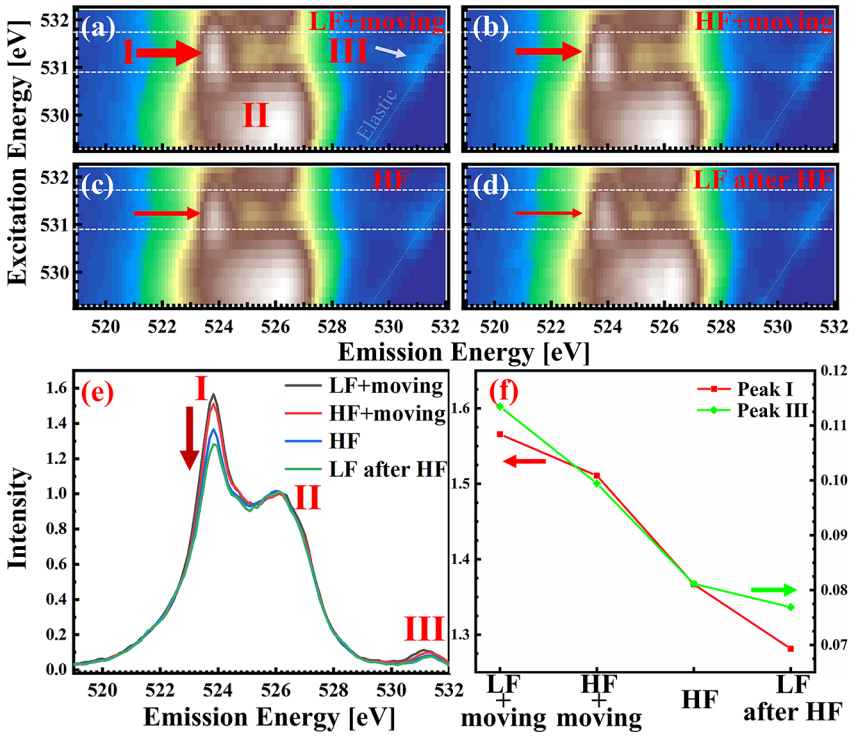

Figure 3. O K-edge mRIXS of the 4.8 V fully charged $Li_{1.144}Ni_{0.136}Mn_{0.544}Co_{0.136}O_2$ electrode at four different irradiation exposure conditions: (a) low X-ray flux (4.5×10^{11} pps) with sample rastering (LF + moving), (b) high flux (2.0×10^{12} pps) with sample rastering (HF + moving), (c) high flux with stationary sample (HF), and (d) low flux with stationary sample (LF after HF) on the same irradiation spot as that for panel c. (e) Integrated mRIXS intensity within the energy window of 530.9 to 531.7 eV excitation energies (between the dashed white lines). The spectra are all normalized to peak (II) for direct comparisons. (f) Summary of the heights of peaks I and III with each test configuration, with low to high radiation dose from left to right.

flux mode, is ~45 min. The oxygen redox reactions in $Li_{1.144}Ni_{0.136}Mn_{0.544}Co_{0.136}O_2$ have been studied in great detail in many previous mRIXS reports.[11,14,15,17,34,35] The typical electrochemical profile is presented in Figure 1a. This work focuses on the two end members of samples at the fully delithiated (charged) and lithiated states.

The O-K mRIXS results of three representative samples, the pristine, charged, and discharged electrodes, are presented in Figure 1b–d. These are typical mRIXS data collected from rastering samples with the LF (4.5×10^{11}) mode. Overall, several intensity packets could be seen. First, broad features with 524–527 eV emission energy across a large range of excitation energies are from the strong TM-O hybridization (II marked in Figure 1c).[17] This feature gets enhanced at the charged state due to the enhancement of the hybridization at highly oxidized states, corresponding to the O-K XAS pre-edge feature enhancement upon charging.[7,10] Second, at the charged state, a new feature emerges around 530–532 excitation energy and around 523.8 eV emission energy (I in Figure 1c), with another concurrent enhancement of the intensity close to the elastic line at the same excitation energy (III in Figure 1c). Both features, I and III, are signatures of oxidized oxygen states[17] and disappear in the discharged state (Figure 1d), indicating a reversible oxygen redox reaction. Again, these mRIXS results are consistent with many previous reports of Li-rich layered materials.[11,14,15,17,34,35] We now focus on the evolution of the features upon different irradiation levels.

We first evaluate the lithiated (pristine or discharged) state, where no oxidized oxygen feature is observed. Figure 2 shows the results of tests for four different irradiation configurations: LF with sample rastering, that is, the lowest dose with a constantly changing exposure spot (Figure 2a); HF with sample rastering (Figure 2b); HF with a stationary sample (Figure 2c); and LF with the sample position unchanged after the HF (Figure 2d). Therefore, the X-ray dose level keeps increasing from Figure 2a–d. The reason for collecting the data in Figure 2d at the LF mode is to obtain the same energy resolution as that for Figure 2a to make sure nothing is missed due to the relatively worse resolution with the HF (large slit sizes) modes.

As shown in Figure 2, no variation of the mRIXS signal could be observed. None of the features of oxidized oxygen, that is, features I or III in Figure 1c, emerges at any of these X-ray exposure conditions. The intensity around the excitation energy window of the oxidized oxygen features (white dashed lines in Figure 2a–d) is integrated and plotted in Figure 2e. All spectra in Figure 2e overlap, showing negligible difference, which indicates that no oxidized oxygen feature shows up in the mRIXS of the lithiated $Li_{1.144}Ni_{0.136}Mn_{0.544}Co_{0.136}O_2$ electrode, even with the highest flux exposure with stationary samples. These results show that X-ray irradiation cannot induce oxidized oxygen in the lithiated sample.

The situation with the fully charged $Li_{1.144}Ni_{0.136}Mn_{0.544}Co_{0.136}O_2$ is a bit more complex because the features from oxidized oxygen, I and III, could already be observed with the LF and rastering mode (Figures 1c and 3a). One may argue that the sample may be radiation-damaged, even with the minimum amount of X-ray dose (LF + rastering). However, if the oxidized oxygen was from radiation damage, then the signals should be enhanced, or at least remain the same, by increasing the X-ray irradiation. Therefore, we performed the same set of four irradiation

https://dx.doi.org/10.1021/acs.jpclett.0c03639
J. Phys. Chem. Lett. 2021, 12, 1138–1143

tests, as described above for the lithiated sample, with the focus on the intensity variation of features I and III.

As shown in Figure 3, the intensity of features I and III is strong in Figure 3a with the lowest dose and becomes weakened in Figure 3d with the strongest dose. Note that data in Figure 3a,d are collected with the same resolution (LF mode), and the only difference is the radiation dose. Figure 3e provides a more direct comparison by integrating the mRIXS intensity within the excitation energy window of the oxidized oxygen features. The spectra show a monotonic decrease in the intensity of features I and III upon the increasing radiation dose. It also shows that with sample rastering, the significant increase in the incident X-ray flux from the LF (4.5×10^{11} pps) to the HF (2.0×10^{12} pps) modes introduces only a small amount of signal decrease (Figure 3b,e). However, if the sample remains stationary, then a significant drop in intensity is observed (Figure 3c,e). Figure 3f plots the variation in the peak intensity of features I and III upon the different steps of our irradiation tests. This mRIXS intensity variation is qualitatively consistent with our previous finding in the quick RIXS cut,[34] with the oxidized oxygen feature intensity decreasing upon irradiation dose.

In summary, by studying the mRIXS feature variation of $Li_{1.144}Ni_{0.136}Mn_{0.544}Co_{0.136}O_2$ in both lithiated and delithiated states upon different irradiation levels, we unambiguously confirm that the oxidized oxygen features revealed by mRIXS in the charged electrode are not from the soft X-ray radiation damage effect. For the delithiated electrode, increasing the X-ray dose leads to a decrease in the oxidized oxygen feature intensity; however, the radiation effect could be largely suppressed by sample rastering during data collection, even with a high flux. The results suggest that the oxidized oxygen features observed in the battery electrodes through mRIXS are intrinsic and could at most be quantitatively underestimated if the irradiation dose is not carefully controlled.

It is interesting to revisit the distinct behaviors of the irradiation effects in different systems: The $LiAlO_2$ and $KMnO_4$ systems display an oxygen oxidation process upon irradiation;[33−35] in sharp contrast, oxidized oxygen systems like Li_2O_2[8] and the charged Li-rich electrodes here go through an oxygen reduction process upon irradiation. It was the cross-use of these distinct radiation damage behaviors that led to the confusion,[32] which deserves to be further clarified. In general, radiation damage has long been a very complex issue that could arise from many effects, such as the bombardment from the secondary electrons, the heating, the excitations from bonding to antibonding states, and so on. However, chemical changes, as focused on in the experiments here, mostly take place in the form of a photon reduction process by irradiation. The key question becomes the choice of the active site for the photon reduction, that is, the weak point for radiation damage. If radiation damage takes place in a typical oxide system with a stable full 2p shell O^{2-} state, then it is easier for the photon reduction to target the metal element, for example, Al^{3+}/Mn^{7+} in $LiAlO_2/KMnO_4$, leading to the reduction of the metal element, which then triggers the oxygen oxidization or even the release of oxygen gas.[33] However, in a system with oxidized oxygen, for example, peroxides and charged electrodes with oxidized oxygen, if the radiation damage takes place, then photon reduction will naturally target the oxidized oxygen and reduce it to the stable O^{2-} state. It is interesting to note that the irradiation effect on the surface of the $LiAlO_2$ displays a nonmonotonic intensity variation due to the loss of the O_2 molecules on the surface, but its bulk oxygen displays a monotonic change in the radiation damage signals.[34] This implies that the oxidized oxygen states could behave differently in the near-surface region and in the bulk. We note that the oxidized oxygen signals found in the mRIXS of charged Li-rich electrodes only correspond to bulk signals away from the surface region.[14] Therefore, radiation damage does not lead to universal behaviors in different oxide systems and may even lead to different surface and bulk behaviors for the same material.

It is important to note that although RIXS provides superior chemical sensitivity over traditional spectroscopic techniques,[10] it is a photon-hungry techniques due to its low statistics, so it is important to clarify the possible radiation damage effect in studies of chemical systems. The in situ resonant inelastic X-ray scattering (iRIXS) system used in this study was specifically designed for studying sensitive chemical systems with ultrahigh efficiency RIXS spectrometers and a compromised resolution.[12] So a relatively low flux level could be used, as in many previous studies. The radiation damage does become a concern and deserves careful evaluation if the flux is high or if the beam size is small for achieving high-energy resolution in RIXS. In particular, the next-generation synchrotron light sources based on diffraction-limited rings (DLRs) greatly improve the X-ray coherency, which will significantly increase the X-ray brightness through focusing optics like zone plates. Caution and further studies on irradiation effects thus become critical for obtaining reliable results on chemical systems because the most active and interesting sites could often be the most prone to radiation damage.

Another related technical challenge of using RIXS as a chemical probe is that whereas we show that maintaining an itinerary sample could be effective in suppressing the radiation damage, such an approach completely loses the spatial information. For the studies of oxidized oxygen states in battery electrodes, this is preferred for obtaining an averaged redox state. However, many chemical studies require spatial resolution. The only solution seems to be the imaging mode without the need for significant beam focusing.[36] We hope that this work also raises these technical challenges in the chemistry, materials, and spectroscopic fields in further developments of the high-efficiency RIXS technique, especially with spatial and temporal resolution, as a superior tool for studying chemical transformations.

AUTHOR INFORMATION

Corresponding Authors

Louis F. J. Piper − *Department of Physics, Applied Physics & Astronomy and Materials Science & Engineering, Binghamton University, Binghamton, New York 13902, United States; WMG, University of Warwick, Coventry CV47AL, United Kingdom;* orcid.org/0000-0002-3421-3210; Email: louis.piper@warwick.ac.uk

Zhi Liu − *State Key Laboratory of Functional Materials for Informatics, Shanghai Institute of Microsystem and Information Technology, Chinese Academy of Sciences, Shanghai 200050, China; University of Chinese Academy of Sciences, Beijing 100049, China; School of Physical Science and Technology, ShanghaiTech University, Shanghai 201210, China;* orcid.org/0000-0002-8973-6561; Email: liuzhi@shanghaitech.edu.cn

https://dx.doi.org/10.1021/acs.jpclett.0c03639
J. Phys. Chem. Lett. 2021, 12, 1138−1143

Wanli Yang − *Advanced Light Source, Lawrence Berkeley National Laboratory, Berkeley, California 94720, United States;* orcid.org/0000-0003-0666-8063; Email: wlyang@lbl.gov

Authors

Qingtian Li − *State Key Laboratory of Functional Materials for Informatics, Shanghai Institute of Microsystem and Information Technology, Chinese Academy of Sciences, Shanghai 200050, China; University of Chinese Academy of Sciences, Beijing 100049, China; Advanced Light Source, Lawrence Berkeley National Laboratory, Berkeley, California 94720, United States*

Zachary W. Lebens-Higgins − *Department of Physics, Applied Physics & Astronomy, Binghamton University, Binghamton, New York 13902, United States*

Yixuan Li − *Department of NanoEngineering, University of California, San Diego, La Jolla, California 92093, United States*

Ying Shirley Meng − *Department of NanoEngineering and Materials Science and Engineering, University of California, San Diego, La Jolla, California 92093, United States*

Yi-de Chuang − *Advanced Light Source, Lawrence Berkeley National Laboratory, Berkeley, California 94720, United States;* orcid.org/0000-0002-2773-3840

Complete contact information is available at: https://pubs.acs.org/10.1021/acs.jpclett.0c03639

Notes

The authors declare no competing financial interest.

■ ACKNOWLEDGMENTS

The Advanced Light Source is supported by the Director, Office of Science, Office of Basic Energy Sciences, of the U.S. Department of Energy under contract no. DE-AC02-05CH11231. This work was also supported as part of the NorthEast Center for Chemical Energy Storage (NECCES), an Energy Frontier Research Center funded by the U.S. Department of Energy, Office of Science, Office of Basic Energy Sciences under award no. DE-SC0012583. Q.L. and Z.L. are supported by National Natural Science Foundation of China (21802096, 22072093, 21832004).

■ REFERENCES

(1) Sathiya, M.; Rousse, G.; Ramesha, K.; Laisa, C. P.; Vezin, H.; Sougrati, M. T.; Doublet, M. L.; Foix, D.; Gonbeau, D.; Walker, W.; et al. Reversible Anionic Redox Chemistry in High-Capacity Layered-Oxide Electrodes. *Nat. Mater.* **2013**, *12* (9), 827−35.

(2) Grimaud, A.; Hong, W. T.; Shao-Horn, Y.; Tarascon, J. M. Anionic Redox Processes for Electrochemical Devices. *Nat. Mater.* **2016**, *15* (2), 121−6.

(3) Assat, G.; Tarascon, J.-M. Fundamental Understanding and Practical Challenges of Anionic Redox Activity in Li-Ion Batteries. *Nature Energy* **2018**, *3* (5), 373−386.

(4) Li, B.; Xia, D. Anionic Redox in Rechargeable Lithium Batteries. *Adv. Mater.* **2017**, *29* (48), 1701054.

(5) Yang, W. Oxygen Release and Oxygen Redox. *Nat. Energy* **2018**, *3* (8), 619−620.

(6) Lebens-Higgins, Z. W.; Chung, H.; Zuba, M. J.; Rana, J.; Li, Y.; Faenza, N. V.; Pereira, N.; McCloskey, B. D.; Rodolakis, F.; Yang, W.; et al. How Bulk Sensitive Is Hard X-ray Photoelectron Spectroscopy: Accounting for the Cathode-Electrolyte Interface When Addressing Oxygen Redox. *J. Phys. Chem. Lett.* **2020**, *11* (6), 2106−2112.

(7) Roychoudhury, S.; Qiao, R.; Zhuo, Z.; Li, Q.; Lyu, Y.; Kim, J. H.; Liu, J.; Lee, E.; Polzin, B. J.; Guo, J.; et al. Deciphering the Oxygen Absorption Pre-Edge: A Caveat on Its Application for Probing Oxygen Redox Reactions in Batteries. *Energy & Environmental Materials* **2020**, DOI: 10.1002/eem2.12119.

(8) Qiao, R.; Chuang, Y. D.; Yan, S.; Yang, W. Soft X-ray Irradiation Effects of Li_2O_2, Li_2Co_3 and Li_2O Revealed by Absorption Spectroscopy. *PLoS One* **2012**, *7* (11), No. e49182.

(9) Ruckman, M. W.; Chen, J.; Qiu, S. L.; Kuiper, P.; Strongin, M.; Dunlap, B. I. Interpreting the near Edges of O_2 and O_2^- in Alkali-Metal Superoxides. *Phys. Rev. Lett.* **1991**, *67* (18), 2533−2536.

(10) Yang, W.; Devereaux, T. P. Anionic and Cationic Redox and Interfaces in Batteries: Advances from Soft X-ray Absorption Spectroscopy to Resonant Inelastic Scattering. *J. Power Sources* **2018**, *389*, 188−197.

(11) Wu, J.; Yang, Y.; Yang, W. Advances in Soft X-ray RIXS for Studying Redox Reaction States in Batteries. *Dalton Trans* **2020**, *49*, 13519−13527.

(12) Qiao, R.; Li, Q.; Zhuo, Z.; Sallis, S.; Fuchs, O.; Blum, M.; Weinhardt, L.; Heske, C.; Pepper, J.; Jones, M.; et al. High-Efficiency in Situ Resonant Inelastic X-ray Scattering (iRIXS) Endstation at the Advanced Light Source. *Rev. Sci. Instrum.* **2017**, *88* (3), 033106.

(13) Dai, K.; Wu, J.; Zhuo, Z.; Li, Q.; Sallis, S.; Mao, J.; Ai, G.; Sun, C.; Li, Z.; Gent, W. E.; et al. High Reversibility of Lattice Oxygen Redox Quantified by Direct Bulk Probes of Both Anionic and Cationic Redox Reactions. *Joule* **2019**, *3* (2), 518−541.

(14) Gent, W. E.; Lim, K.; Liang, Y.; Li, Q.; Barnes, T.; Ahn, S. J.; Stone, K. H.; McIntire, M.; Hong, J.; Song, J. H.; et al. Coupling between Oxygen Redox and Cation Migration Explains Unusual Electrochemistry in Lithium-Rich Layered Oxides. *Nat. Commun.* **2017**, *8* (1), 2091.

(15) Xu, J.; Sun, M.; Qiao, R.; Renfrew, S. E.; Ma, L.; Wu, T.; Hwang, S.; Nordlund, D.; Su, D.; Amine, K.; et al. Elucidating Anionic Oxygen Activity in Lithium-Rich Layered Oxides. *Nat. Commun.* **2018**, *9* (1), 947.

(16) Lebens-Higgins, Z. W.; Faenza, N. V.; Radin, M. D.; Liu, H.; Sallis, S.; Rana, J.; Vinckeviciute, J.; Reeves, P. J.; Zuba, M. J.; Badway, F.; et al. Revisiting the Charge Compensation Mechanisms in $LiNi_{0.8}Co_{0.2-y}Al_yO_2$ Systems. *Mater. Horiz.* **2019**, *6* (10), 2112−2123.

(17) Wu, J.; Li, Q.; Sallis, S.; Zhuo, Z.; Gent, W.; Chueh, W.; Yan, S.; Chuang, Y.-d.; Yang, W. Fingerprint Oxygen Redox Reactions in Batteries through High-Efficiency Mapping of Resonant Inelastic X-ray Scattering. *Condensed Matter* **2019**, *4* (1), 5.

(18) Zhuo, Z.; Pemmaraju, C. D.; Vinson, J.; Jia, C.; Moritz, B.; Lee, I.; Sallies, S.; Li, Q.; Wu, J.; Dai, K.; et al. Spectroscopic Signature of Oxidized Oxygen States in Peroxides. *J. Phys. Chem. Lett.* **2018**, *9* (21), 6378−6384.

(19) Zhuo, Z.; Liu, Y. S.; Guo, J.; Chuang, Y. D.; Pan, F.; Yang, W. Full Energy Range Resonant Inelastic X-ray Scattering of O_2 and CO_2: Direct Comparison with Oxygen Redox State in Batteries. *J. Phys. Chem. Lett.* **2020**, *11* (7), 2618−2623.

(20) Luo, K.; Roberts, M. R.; Hao, R.; Guerrini, N.; Pickup, D. M.; Liu, Y. S.; Edstrom, K.; Guo, J.; Chadwick, A. V.; Duda, L. C.; et al. Charge-Compensation in 3d-Transition-Metal-Oxide Intercalation Cathodes through the Generation of Localized Electron Holes on Oxygen. *Nat. Chem.* **2016**, *8* (7), 684−91.

(21) House, R. A.; Maitra, U.; Perez-Osorio, M. A.; Lozano, J. G.; Jin, L.; Somerville, J. W.; Duda, L. C.; Nag, A.; Walters, A.; Zhou, K. J.; et al. Superstructure Control of First-Cycle Voltage Hysteresis in Oxygen-Redox Cathodes. *Nature* **2020**, *577* (7791), 502−508.

(22) Wu, J.; Zhuo, Z.; Rong, X.; Dai, K.; Lebens-Higgins, Z.; Sallis, S.; Pan, F.; Piper, L. F. J.; Liu, G.; Chuang, Y. D.; et al. Dissociate Lattice Oxygen Redox Reactions from Capacity and Voltage Drops of Battery Electrodes. *Sci. Adv.* **2020**, *6* (6), No. eaaw3871.

(23) Chen, D.; Wu, J.; Papp, J. K.; McCloskey, B. D.; Yang, W.; Chen, G. Role of Redox-Inactive Transition-Metals in the Behavior of Cation-Disordered Rocksalt Cathodes. *Small* **2020**, *16* (22), No. 2000656.

(24) Lee, G. H.; Wu, J.; Kim, D.; Cho, K.; Cho, M.; Yang, W.; Kang, Y. M. Reversible Anionic Redox Activities in Conventional $LiNi_{1/3}Co_{1/3}Mn_{1/3}O_2$ Cathodes. *Angew. Chem., Int. Ed.* **2020**, *59* (22), 8681−8688.
(25) Li, N.; Wu, J.; Hwang, S.; Papp, J. K.; Kan, W. H.; Zhang, L.; Zhu, C.; McCloskey, B. D.; Yang, W.; Tong, W. Enabling Facile Anionic Kinetics through Cationic Redox Mediator in Li-Rich Layered Cathodes. *ACS Energy Letters* **2020**, *5*, 3535−3543.
(26) Li, N.; Sallis, S.; Papp, J. K.; Wei, J.; McCloskey, B. D.; Yang, W.; Tong, W. Unraveling the Cationic and Anionic Redox Reactions in a Conventional Layered Oxide Cathode. *ACS Energy Letters* **2019**, *4*, 2836−2842.
(27) Wu, J.; Zhang, X.; Zheng, S.; Liu, H.; Wu, J.; Fu, R.; Li, Y.; Xiang, Y.; Liu, R.; Zuo, W.; et al. Tuning Oxygen Redox Reaction through the Inductive Effect with Proton Insertion in Li-Rich Oxides. *ACS Appl. Mater. Interfaces* **2020**, *12* (6), 7277−7284.
(28) Zhao, E.; Li, Q.; Meng, F.; Liu, J.; Wang, J.; He, L.; Jiang, Z.; Zhang, Q.; Yu, X.; Gu, L.; et al. Stabilizing the Oxygen Lattice and Reversible Oxygen Redox Chemistry through Structural Dimensionality in Lithium-Rich Cathode Oxides. *Angew. Chem., Int. Ed.* **2019**, *58* (13), 4323−4327.
(29) Dai, K.; Mao, J.; Zhuo, Z.; Feng, Y.; Mao, W.; Ai, G.; Pan, F.; Chuang, Y.-d.; Liu, G.; Yang, W. Negligible Voltage Hysteresis with Strong Anionic Redox in Conventional Battery Electrode. *Nano Energy* **2020**, *74*, 104831.
(30) Wu, J.; Shen, Z.-x.; Yang, W. Redox Mechanism in Na-Ion Battery Cathodes Probed by Advanced Soft X-ray Spectroscopy. *Front. Chem.* **2020**, *8*, 816.
(31) Hong, J.; Gent, W. E.; Xiao, P.; Lim, K.; Seo, D. H.; Wu, J.; Csernica, P. M.; Takacs, C. J.; Nordlund, D.; Sun, C. J.; et al. Metal-Oxygen Decoordination Stabilizes Anion Redox in Li-Rich Oxides. *Nat. Mater.* **2019**, *18* (3), 256−265.
(32) Radin, M. D.; Vinckeviciute, J.; Seshadri, R.; Van der Ven, A. Manganese Oxidation as the Origin of the Anomalous Capacity of Mn-Containing Li-Excess Cathode Materials. *Nat. Energy* **2019**, *4* (8), 639−646.
(33) Hetaba, W.; Mogilatenko, A.; Neumann, W. Electron Beam-Induced Oxygen Desorption in Gamma-$LiAlO_2$. *Micron* **2010**, *41* (5), 479−483.
(34) Lebens-Higgins, Z. W.; Vinckeviciute, J.; Wu, J.; Faenza, N. V.; Li, Y.; Sallis, S.; Pereira, N.; Meng, Y. S.; Amatucci, G. G.; Der Ven, A. V.; et al. Distinction between Intrinsic and X-ray-Induced Oxidized Oxygen States in Li-Rich 3d Layered Oxides and $LiAlO_2$. *J. Phys. Chem. C* **2019**, *123* (21), 13201−13207.
(35) Gent, W. E.; Abate, I. I.; Yang, W.; Nazar, L. F.; Chueh, W. C. Design Rules for High-Valent Redox in Intercalation Electrodes. *Joule* **2020**, *4* (7), 1369−1397.
(36) Chuang, Y.-D.; Feng, X.; Glans-Suzuki, P.-A.; Yang, W.; Padmore, H.; Guo, J. A Design of Resonant Inelastic X-ray Scattering (RIXS) Spectrometer for Spatial- and Time-Resolved Spectroscopy. *J. Synchrotron Radiat.* **2020**, *27* (3), 695−707.

https://dx.doi.org/10.1021/acs.jpclett.0c03639
J. Phys. Chem. Lett. 2021, 12, 1138−1143